Petroleum Science 22 (2025) 2977–2991

Contents lists available at ScienceDirect

Petroleum Science

journal homepage: www.keaipublishing.com/en/journals/petroleum-science

Original Paper

Multiscale investigation into EOR mechanisms and influencing factors for CO_2-WAG injection in heterogeneous sandy conglomerate reservoirs using NMR technology

Jun-Rong Liu [a, b, c], Deng-Feng Zhang [a, b, c], Shu-Yang Liu [a, b, c, *], Run-Dong Gong [a, b, c], Li Wang [a, b, c]

[a] School of Petroleum Engineering, China University of Petroleum (East China), Qingdao, 266580, Shandong, PR China
[b] Key Laboratory of Unconventional Oil & Gas Development (China University of Petroleum (East China)), Ministry of Education, Qingdao, 266580, Shandong, PR China
[c] State Key Laboratory of Deep Oil and Gas, China University of Petroleum (East China), Qingdao, 266580, Shandong, PR China

A R T I C L E I N F O

Article history:
Received 9 October 2024
Received in revised form
1 April 2025
Accepted 1 April 2025
Available online 2 April 2025

Edited by Yan-Hua Sun

Keywords:
Multiscale investigation
Heterogeneous reservoir
CO_2-WAG displacement
EOR mechanism
NMR

A B S T R A C T

The sandy conglomerate reservoir is tight and exhibits strong heterogeneity, rendering conventional water flooding and gas drive methods inefficient and challenging for the effective development. CO_2 water alternating gas (CO_2-WAG) injection as an effective enhanced oil recovery (EOR) method has been applied in heterogeneous reservoirs. Simultaneously, it facilitates carbon sequestration, contributing to the green and low-carbon transformation of energy. However, the EOR mechanisms and influencing factors are still unclear for the development of heterogeneous sandy conglomerate reservoirs. In this paper, we conducted core flooding experiments combined nuclear magnetic resonance (NMR) technology to investigate EOR mechanisms of the CO_2-WAG injection on the multiscale (reservoir, layer, and pore). The study compared multiscale oil recovery in sandy conglomerate reservoirs under both miscible and immiscible conditions, while also analyzing the effects of water–gas ratio and injection rate. In the immiscible state, the CO_2-WAG displacement achieves an oil recovery of approximately 22.95%, representing a 7.82% increase compared to CO_2 flooding. This method effectively inhibits CO_2 breakthrough in high-permeability layers while enhancing the oil recovery in medium- and low-permeability layers. Furthermore, CO_2-WAG displacement improves the microscopic oil displacement efficiency within mesopores and micropores. As the water–gas ratio increases, the total oil recovery rises, with enhanced oil recovery in low-permeability layers and micropores. Moreover, a gradual increase in injection rate leads to a decrease in total oil recovery, but it leads to an increase in oil recovery from low-permeability sandy conglomerate layers and micropores. In the miscible state, the displacement efficiency of CO_2-WAG is significantly enhanced, the total oil recovery three times higher than that in the immiscible state. In particular, the oil recovery from low permeability layers and micropores has further improved. Additionally, experimental results indicate that parameters such as water–gas ratio and injection rate do not significantly affect the oil recovery of CO_2-WAG miscible displacement. Therefore, maintaining the reservoir pressure above the minimum miscible pressure is the key to maximizing ultimate recovery factor in these reservoirs.

1. Introduction

In the context of the low-carbon energy transition, CO_2 flooding is an effective technology that not only enhances oil recovery but also facilitates carbon sequestration (Henni, 2014; Liu et al., 2022a; Singh, 2018; Zhang et al., 2023). Current research indicates that CO_2 possesses high permeability, allowing it to enter micropores easily

* Corresponding author.
E-mail address: liu.shuyang@upc.edu.cn (S.-Y. Liu).
Peer review under the responsibility of China University of Petroleum (Beijing).

https://doi.org/10.1016/j.petsci.2025.04.004

and making its injection into tight reservoirs feasible. The enhanced oil recovery (EOR) mechanisms of this technology primarily include crude oil expansion, viscosity reduction, and miscibility (Al-Saedi et al., 2019; Hu et al., 2019; Lan et al., 2019; Qian et al., 2019; Xu et al., 2022). Numerous oilfield practices have demonstrated that the CO_2 flooding can improve oil recovery (Guo and Xu, 2014; Liu et al., 2017; Liu et al., 2022b; Wang et al., 2013). Additionally, this process sequesters CO_2 underground, contributing to carbon neutrality (Chen et al., 2016; Tian et al., 2022; Yu et al., 2022).

However, CO_2 flooding still faces several challenges. In highly heterogeneous reservoirs, oil recovery is often limited due to early CO_2 breakthrough, severe gas channeling, and low sweep efficiency (Du et al., 2020; Jiang et al., 2023; Wang et al., 2023). Similarly, conventional water flooding in such reservoirs encounters its own set of issues, including injection difficulties, low recovery rates, and high flow resistance. These factors lead to slow propagation of pressure and rapid depletion of reservoir energy (Afzali et al., 2018; Chen et al., 2010; Nezhad et al., 2006; Odesa, 2018).

To address these technical challenges, CO_2 water alternating gas (CO_2-WAG) injection, an effective EOR method, has been applied in heterogeneous reservoirs. CO_2-WAG displacement combines the advantages of both water and gas flooding, maintaining injectivity while suppressing gas channeling (Ramachandran et al., 2010). To investigate the underlying mechanisms, many scholars and experts have conducted extensive experimental research.

Kulkarni and Rao (2005) compared the performance of WAG flooding and continuous gas injection, concluding that WAG flooding can achieve a broad sweep area and a higher displacement efficiency. Similarly, Masalmeh et al. (2022) evaluated the gas injection in carbonate reservoirs and found that WAG flooding, when applied after gas injection, further reduces the residual oil saturation and enhances the oil recovery. However, both studies were conducted using homogeneous cores, which do not fully represent the varying degrees of heterogeneity found in actual reservoirs.

To address this, Zhao et al. (2019) explored the mechanisms by which CO_2-WAG enhances oil recovery in heterogeneous reservoirs. They compared different injection methods—water flooding, gas flooding, and WAG—on oil recovery efficiency in heterogeneous carbonate reservoirs. Their results show that WAG flooding significantly lowers the water cut compared to water flooding and maintains a stable gas–oil ratio, delaying gas breakthrough. Among these methods, WAG flooding achieves the highest oil recovery, followed by continuous gas flooding and water flooding. While Zhao et al. (2019)'s study considered heterogeneity on the core scale, it focused more on localized heterogeneity and did not fully capture the complexity of entire reservoirs.

Wang et al. (2021) addressed reservoir heterogeneity using parallel cores to simulate interlayer differences, and employed NMR technology to study the effects of various displacement methods on oil recovery. Their findings show that reservoir heterogeneity significantly reduces the efficiency of oil displacement. Moreover, Cui et al. (2022) conducted WAG flooding experiments using vertically and horizontally heterogeneous synthetic cores and found that the residual oil distribution after WAG injection is larger in heterogeneous cores than in homogeneous ones. This occurs because, in the later stages of WAG injection, the gas–water slug diverts toward low-permeability zones, reducing injection efficiency in high-permeability zones and decreasing the overall displacement effect. While both studies used NMR technology to examine the effect of WAG flooding on oil recovery in heterogeneous reservoirs, neither employed NMR to quantitatively analyze oil recovery on the pore scale.

In addition, the miscible state also affects the CO_2-WAG performance. Kulkarni and Rao (2005) found that the miscible CO_2-WAG displacement achieves an oil recovery rate of 60%–70% higher than the immiscible displacement. Furthermore, Cai et al. (2021) used on-line NMR imaging technology to monitor CO_2 displacement in low-permeability sandstone cores under different reservoir pressures. The results show that the oil recovery by miscible flooding (69.4%) is twice more than that by immiscible flooding (32.6%). The studies above suggest that oil recovery by WAG is also influenced by miscible conditions. However, they relied solely on overall recovery factors as evaluation criteria and did not assess heterogeneity on the interlayer or pore scale. Consequently, they could not fully explore the mechanisms of oil displacement by WAG under different miscible conditions on the multiscale.

In this paper, we explored the EOR mechanism of CO_2-WAG on the multiscales—reservoir, layer, and pore—using core experiments combined with NMR technology. We also analyzed the influence of displacement parameters such as injection rate and water–gas ratio in both miscible and immiscible states.

2. Experimental

2.1. Experimental materials

The target reservoir in this study is a sandy conglomerate reservoir, which can be classified into coarse sandstone, conglomerate-bearing sandstone, and sandy conglomerate layers based on the sand-to-gravel ratio (as shown in Fig. 1). The permeability and porosity of these layers are very different, and the reservoir exhibits strong heterogeneity. The reservoir temperature and pressure are about 70 °C and 20–27 MPa.

In this experiment, cylindrical rock samples were cut from the three distinct layers, and their permeability and porosity were measured using a pulse-decay permeameter and a porosity meter. The basic physical properties are presented in Table 1. Core samples 1–5 are coarse sandstone samples with permeability of 100–150 mD and porosity of 0.12–0.17. Core samples 6–9 are conglomerate-bearing sandstone samples with permeability of 10–50 mD and porosity of 0.1–0.12. Core samples 10–14 are sandy conglomerate samples with permeability of 0.1–10 mD and porosity of 0.07–0.12. The experimental results indicate a significant difference in permeability across the various layers of the target reservoir.

D_2O (heavy water) with purity of 99.8% was used as the aqueous phase in the experiment because it exhibits no signal in proton NMR detection. This allows the NMR instrument to more effectively track the remaining oil in the core. The viscosity of the heavy water was 1.23 mPa s at experimental temperature, similar to that of H_2O

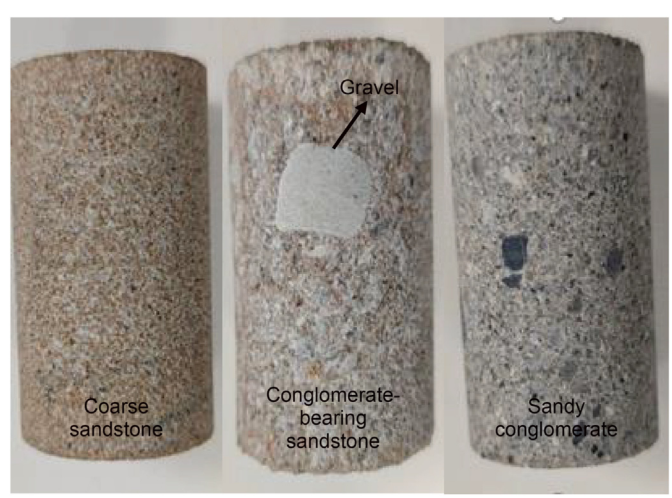

Fig. 1. Experimental core samples.

Table 1
Basic property parameters of experimental cores.

Core type	Core No.	Length, cm	Diameter, cm	Porosity, %	Permeability, mD
Coarse sandstone	1	4.761	2.541	16.41	134.19
	2	4.904	2.528	13.56	122.24
	3	4.806	2.535	13.94	123.56
	4	4.881	2.540	16.63	146.03
	5	4.851	2.456	12.84	142.35
Conglomerate-bearing sandstone	6	4.928	2.465	10.71	30.79
	7	4.979	2.523	10.34	20.43
	8	4.899	2.534	10.65	16.84
	9	4.956	2.512	12.06	10.83
Sandy conglomerate	10	4.863	2.531	7.78	0.68
	11	4.892	2.506	11.52	0.23
	12	4.878	2.527	8.33	1.80
	13	5.214	2.513	9.41	3.22
	14	5.128	2.516	9.23	2.10

(deionized water). The gas used was high-purity CO_2. The experimental oil was sourced from the crude oil in the target reservoir. The viscosity of the crude oil was 5.93 mPa s at 70 °C. The components of the experimental oil were measured using a gas chromatography-mass spectrometry (CG-MS), as detailed in Table 2.

2.2. Experimental setup and procedures

2.2.1. Experimental setup

To investigate EOR mechanisms of CO_2-WAG injection in sandy conglomerate reservoirs, we conducted core displacement experiments coupled with real-time monitoring by NMR instrument. The schematic diagram and image of the experimental setup are shown in Figs. 2 and 3. The experimental setup primarily consists of three components: injection, monitoring, and collection systems. In the injection system, two high-precision piston pumps (manufactured by Vindum Engineering) are used to control three piston-type accumulators to inject water and gas into the core. This is achieved by adjusting two check valves and two three-way valves to ensure stable injection of fluids. In the monitoring system, three core holders are connected in parallel, and the core samples from three different layers are individually placed in separate core holders. Through this design, the heterogeneous reservoir is simulated. The inlet ends of the core holders are connected with a six-way valve, and the outlet ends are connected with another six-way valve. During the experimental process, the cores are scanned using an on-line NMR instrument to monitor the amount and distribution of residual oil. The collection system consists of three gas–liquid separators and a gas flow meter. The volumes of oil and water are measured using the gas–liquid separators, while the volume of outgassing is measured with the gas flow meter.

2.2.2. Experimental procedures

The minimum miscible pressure (MMP) between experimental oil and CO_2 was measured to be 23.1 MPa at the experimental temperature using a slim tube test, the diagram of the experimental setup is shown in Fig. 4.

The specific experimental steps for the slim tube experiment are as follows:

(1) Use anhydrous ethanol to clean the slim tube, syringe, and connecting pipes, ensuring they are free from oil or other contaminants.
(2) Install a thermostatic heating device to heat the experimental system to a temperature of 70 °C.
(3) Inject the experimental oil sample into the slim tube to fully saturate the tube with the oil, and record the volume of the experimental oil sample inside the slim tube.
(4) Slowly inject CO_2 into the slim tube using a high-pressure pump, while monitoring the pressure changes on the pressure gauge and the volume of displaced experimental oil.
(5) Observe the miscibility of CO_2 and experimental oil through the observation window. When a single-phase liquid is formed, record the pressure at this point.
(6) Clean the equipment and repeat the experiment to ensure the reliability of the results.
(7) After the experiment, clean the experimental equipment, process the data, and determine the MMP between CO_2 and experimental oil to be 23.1 MPa.

Table 2
Components of experimental oil.

Carbon number	Mass fraction, %	Carbon number	Mass fraction, %	Carbon number	Mass fraction, %
≤ 6	1.6046	21	2.6140	36	1.1427
7	4.1314	22	2.6094	37	0.9693
8	6.1625	23	2.4135	38	0.9364
9	3.0514	24	2.2826	39	0.9032
10	3.0381	25	2.3611	40	0.8786
11	2.7665	26	2.4086	41	0.7949
12	2.7813	27	2.3982	42	0.7813
13	2.8989	28	2.4061	43	0.7108
14	3.1354	29	2.2997	44	0.7004
15	2.9912	30	2.2997	45	0.6875
16	2.8489	31	2.0077	46	0.6620
17	3.1317	32	1.6752	47	0.5959
18	2.9435	33	1.4773	48	0.5882
19	2.7344	34	1.2871	49	0.5107
20	2.5734	35	1.2535	≥ 50	10.5512

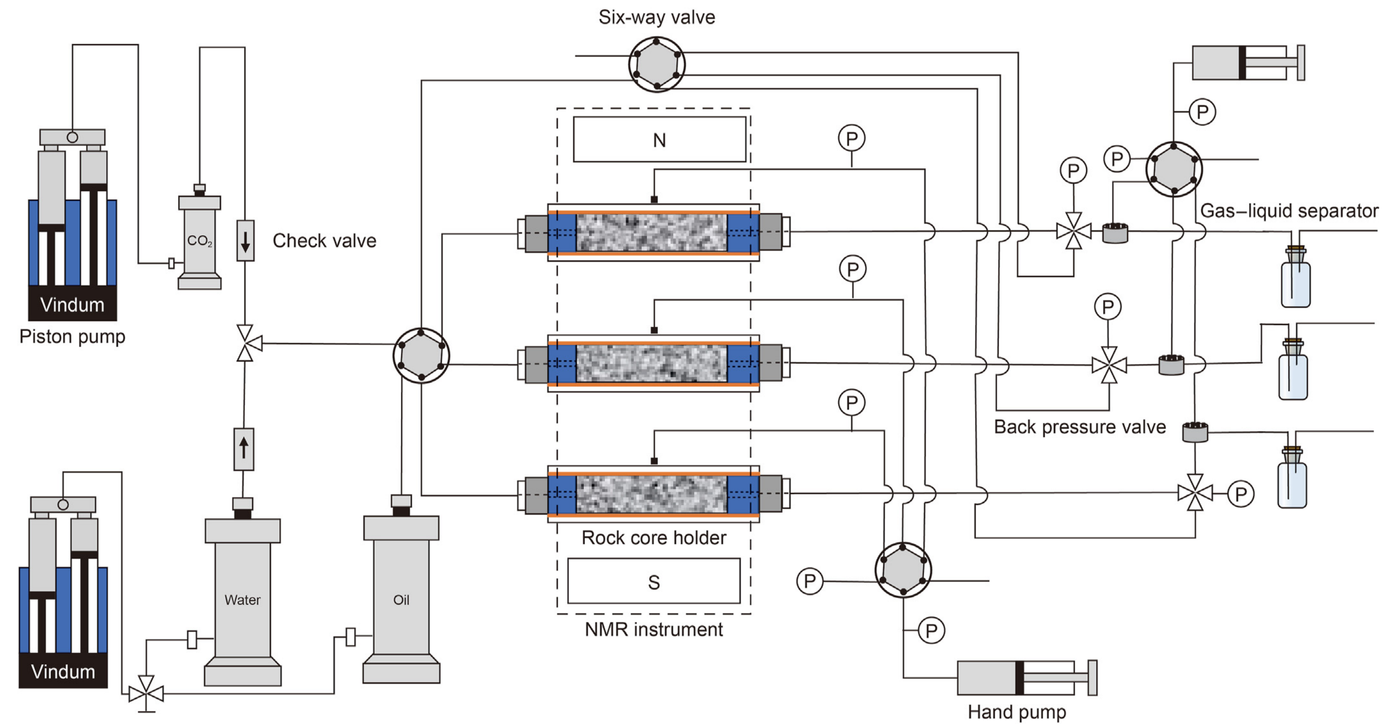

Fig. 2. Schematic diagram of the experimental setup for NMR-assisted CO_2-WAG displacement.

Fig. 3. Image of the experimental system for NMR-assisted CO_2-WAG displacement.

The MMP between experimental oil and CO_2, determined from the slim tube test, was found to be 23.1 MPa, which is close to the reservoir pressure. Therefore, both miscible and immiscible displacement processes may occur in the process of gas injection. To study the oil recovery effects of miscible and immiscible CO_2-WAG injection in sandy conglomerate reservoirs, the experiment was conducted at 20 and 27 MPa, respectively. Additionally, the effect of gas injection rate and gas–water ratio were also studied, the specific experimental schemes are shown in Table 3.

During the core displacement process, real-time measurements can be performed sequentially on the three parallel cores. Before the start of the experiment, adjust the six-way valve to connect the pipeline before and after the core holder, set the constant pressure mode of the pump, adjust the pressure at the outlet end of the core holder, so that the pressure of the whole test system is consistent with the actual reservoir.

The specific experimental steps for the CO_2/CO_2 WAG displacement process are as follows:

(1) After washing with oil, the cores are placed in an oven set at 120 °C and dried for 24 h until completely dry, place these cores in the core holders and apply the set confining pressure.
(2) Heavy water is injected to saturate the cores at a rate of 0.05 mL/min, then inject oil into the cores until no water is produced at the outlet to establish bound water saturation.
(3) Under immiscible and miscible conditions, the back pressure of the three cores is maintained at a constant 20/27 MPa, with the confining pressure set to 24/30 MPa.
(4) The cores are scanned with an NMR device to obtain NMR images and T_2 spectra.
(5) Inject the set amounts of CO_2 and heavy water to perform the CO_2 and CO_2-WAG injection experiments.
(6) When the displacement reaches several key points (initial state, CO_2 breakthrough, and the injection volume of 1, 5, 10 pore volume (PV), the three cores are sequentially scanned to obtain NMR images and dynamic T_2 spectra of the displacement process.
(7) Stop the injection when there is no further oil production.

3. Results and discussion

3.1. EOR mechanisms and influencing factors for CO_2-WAG flooding under immiscible condition

3.1.1. Comparative analysis of recovery performance in CO_2 flooding and CO_2-WAG flooding under immiscible condition

To investigate EOR mechanisms of CO_2-WAG injection in heterogeneous sandy conglomerate reservoirs under immiscible conditions, this study utilized NMR technology to monitor the dynamic

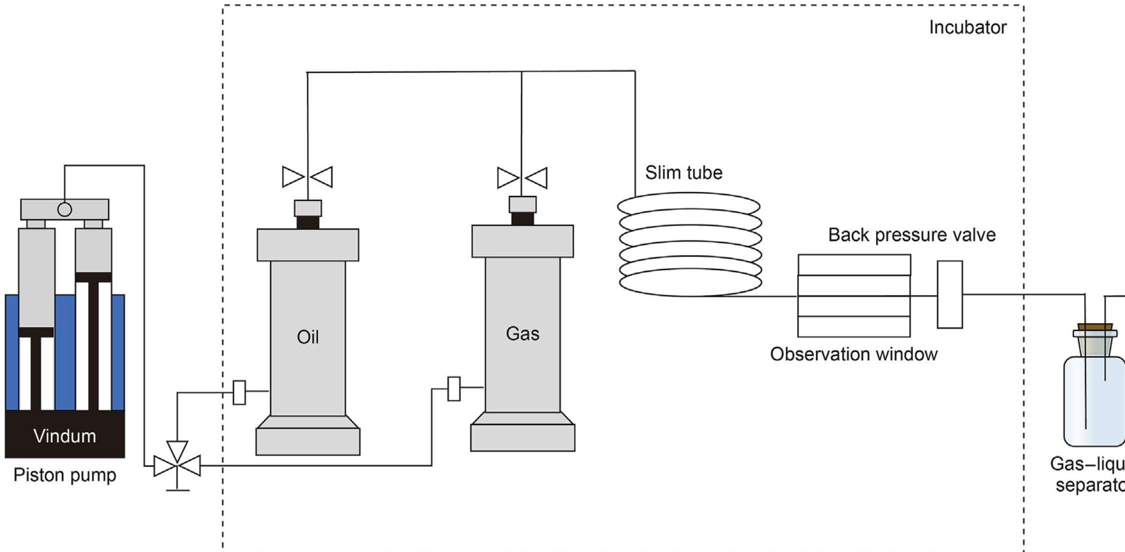

Fig. 4. Schematic diagram of the slim tube test apparatus.

Table 3
Experimental scheme design.

Number	Gas–water ratio	Production pressure, MPa	Gas injection rate, mL/min
1	Pure gas	20	5
2	1:1	20	5
3	1:2	20	5
4	2:1	20	5
5	1:1	20	2
6	1:1	20	0.5
7	Pure gas	27	5
8	1:1	27	5
9	2:1	27	5
10	1:2	27	5
11	1:1	27	2
12	1:1	27	0.5

distribution of residual oil during CO_2 flooding and CO_2-WAG flooding. NMR imaging was performed at several key points (initial state, gas breakthrough, and 1, 5, 10 PV of gas injected into the cores) in the displacement process, and the results are shown in Fig. 5. The experimental water (D_2O) and rock skeleton have no NMR signal (shown in blue in the figure), while the oil generates a stronger NMR signal (shown in red), the NMR image can effectively characterize the distribution of residual oil qualitatively. The dynamic images indicate that a significant amount of residual oil is still trapped in the cores after gas breakthrough. As the displacement continues, the residual oil saturation in the high-permeability coarse sandstone layer decreases significantly, while in the low-permeability sandy conglomerate layer the distribution of residual oil changes slightly. It is observed that in the process of CO_2 displacement and CO_2-WAG displacement, gas preferentially breakthroughs in the high-permeability layer, followed by the medium-permeability layer, and finally the low-permeability layer. However, CO_2-WAG injection can delay gas breakthrough in the low-permeability layer and improve oil recovery in that layer to some extent.

To further quantify the oil recovery effects of the two displacement modes, the dynamic T_2 spectra during displacement were obtained, as shown in Fig. 6. Base on the principle of NMR detection technology, the amount of ^{1}H-containing fluid is proportional to the NMR signal (Liu et al., 2023). In the experiment, only the oil phase contains ^{1}H (heavy water contains ^{2}H), so the amount of residual oil in the core can be characterized by the envelope area of the T_2 spectrum, representing the total amount of NMR signals. Therefore, we measured the NMR signal intensity for oil samples ranging from 1 to 5 mL to establish the relationship between the NMR signal and the oil volume, as depicted in Fig. 7.

The curve demonstrates a strong linear relationship, with a coefficient of determination (R^2) of 0.9993. This robust correlation underscores that NMR signals serve as a dependable indicator of oil variations within the cores. The relationship between NMR signal and oil volume can be expressed as follows:

$$V_{oil} = 0.0003Q - 0.0118 \tag{1}$$

where V_{oil} is the volume of oil in the cores, mL; Q is the NMR signal intensity.

Then, we can calculate the oil recovery as outlined in Eq. (2):

$$R = 1 - \frac{V_r}{V_i} = 1 - \frac{0.0003Q_r - 0.0118}{0.0003Q_i - 0.0118} \tag{2}$$

where V_r is the residual oil volume in the cores after displacement, mL; V_i is the volume of initial saturated oil in the cores, mL; Q_r is the NMR intensity of residual oil in the cores after displacement; Q_i is NMR intensity of the initial saturated oil in the core.

Using Eq. (2) we obtain the total oil recovery of simulated

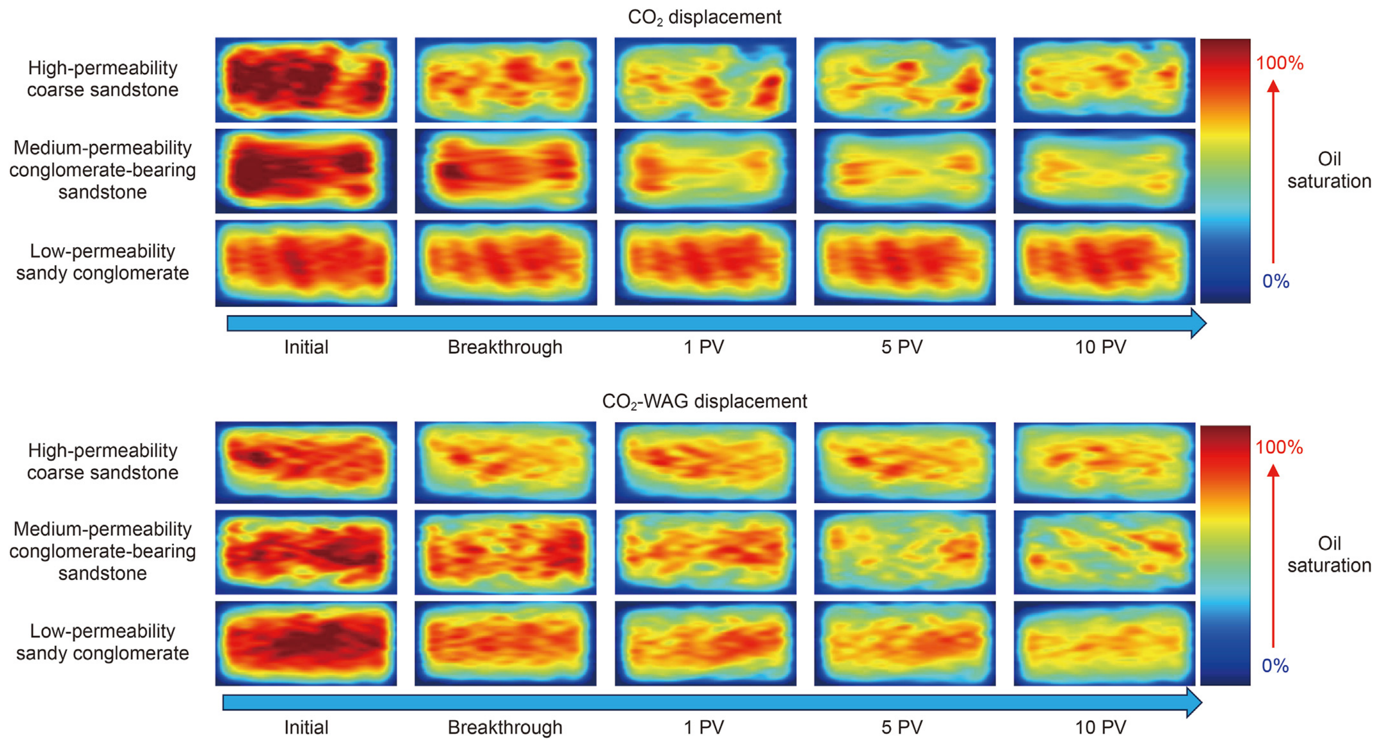

Fig. 5. Dynamic NMR imaging of heterogeneous cores during CO_2 displacement and CO_2-WAG displacement (1:1 water–gas ratio).

heterogeneous reservoirs under different displacement modes, as well as the oil recovery from each layer, as shown in Fig. 8. The results show that compared with CO_2 injection, CO_2-WAG injection can significantly improve the total oil recovery of heterogeneous reservoirs by up to 7.82% (from 15.13% to 22.95%). After the application of CO_2-WAG, the oil recovery from each layer improves, with the low-permeability sandy conglomerate layer showing the greatest enhancement, nearly tripling. Therefore, the EOR mechanism of CO_2-WAG injection in the heterogeneous reservoir primarily involves improving the utilization of oil trapped in the low-permeability sandy conglomerate layer.

To investigate deeper into the microscopic EOR mechanisms of the CO_2-WAG injection on the pore scale, we classified rock pores into three types: micropores, mesopores, macropores according to the relaxation time in the T_2 spectrum. The dynamic T_2 spectrum can reveal the movement of fluids in different pores. This relationship can be expressed as follows (Toumelin et al., 2007):

$$\frac{1}{T_2} = \rho_2 \left(\frac{S}{V}\right)_{\text{pore}} \tag{3}$$

where ρ_2 is the surface relaxation term, m/s; $\frac{S}{V}$ represents the surface-to-volume ratio of the pore, 1/m.

Base on the previous classification criteria, specifically, a relaxation time of 0.01–1 ms indicates a micropore, 1–100 ms corresponds to a mesopores, and 100–10,000 ms defines a micropore. Therefore, the oil recovery on the pore scale can be derived from Eq. (2):

$$R_{\text{i}} = 1 - \frac{V_{\text{ri}}}{V_{\text{ii}}} = 1 - \frac{0.0003Q_{\text{ri}} - 0.0118}{0.0003Q_{\text{ii}} - 0.0118} \tag{4}$$

$$R_{\text{e}} = 1 - \frac{V_{\text{re}}}{V_{\text{ie}}} = 1 - \frac{0.0003Q_{\text{re}} - 0.0118}{0.0003Q_{\text{ie}} - 0.0118} \tag{5}$$

$$R_{\text{a}} = 1 - \frac{V_{\text{ra}}}{V_{\text{ia}}} = 1 - \frac{0.00013Q_{\text{ra}} - 0.0118}{0.0003Q_{\text{ia}} - 0.0118} \tag{6}$$

where R_i, R_e, and R_a are the oil recovery from micropores, mesopores, and macropores; V_{ri}, V_{re}, and V_{ra} are the volumes of residual oil in micropores, mesopores, and macropores after displacement, mL; V_{ii}, V_{ie}, and V_{ia} are the volume of initial saturated oil in micropores, mesopores and macropores, mL; Q_{ri}, Q_{re}, and Q_{ra} are NMR intensity of residual oil in micropores, mesopores, and macropores after displacement; Q_{ii}, Q_{ie}, and Q_{ia} are the NMR intensity of the initial saturated oil in micropores, mesopores, and macropores.

The experimental results are calculated by combining T_2 spectra and Eqs. (4)–(6), as shown in Fig. 9. Compared with CO_2 injection, CO_2-WAG injection improves oil recovery from various types of pores, with the highest increase of 8% observed in micropores. Despite this, the oil recovery from mesopores and micropores remains low. Therefore, the next section will examine the influences of CO_2-WAG production parameters, such as water–gas ratio and injection rate, on oil recovery to provide theoretical guidance for optimizing the CO_2-WAG process.

3.1.2. Impact of water–gas ratio on multiscale oil recovery in CO_2-WAG flooding under immiscible condition

To systematically evaluate the effect of water–gas ratio in the CO_2-WAG process, dynamic NMR imaging was performed to visualize the CO_2-WAG injection with different water–gas ratios (1:2, 1:1, 2:1), as illustrated in Fig. 10. The experimental results reveal that an increase in the water–gas ratio effectively delays gas breakthrough in the high-permeability cores, with corresponding injection volume of 0.26, 0.32, and 0.41 PV, respectively. This indicates that higher water–gas ratio can mitigate gas channeling

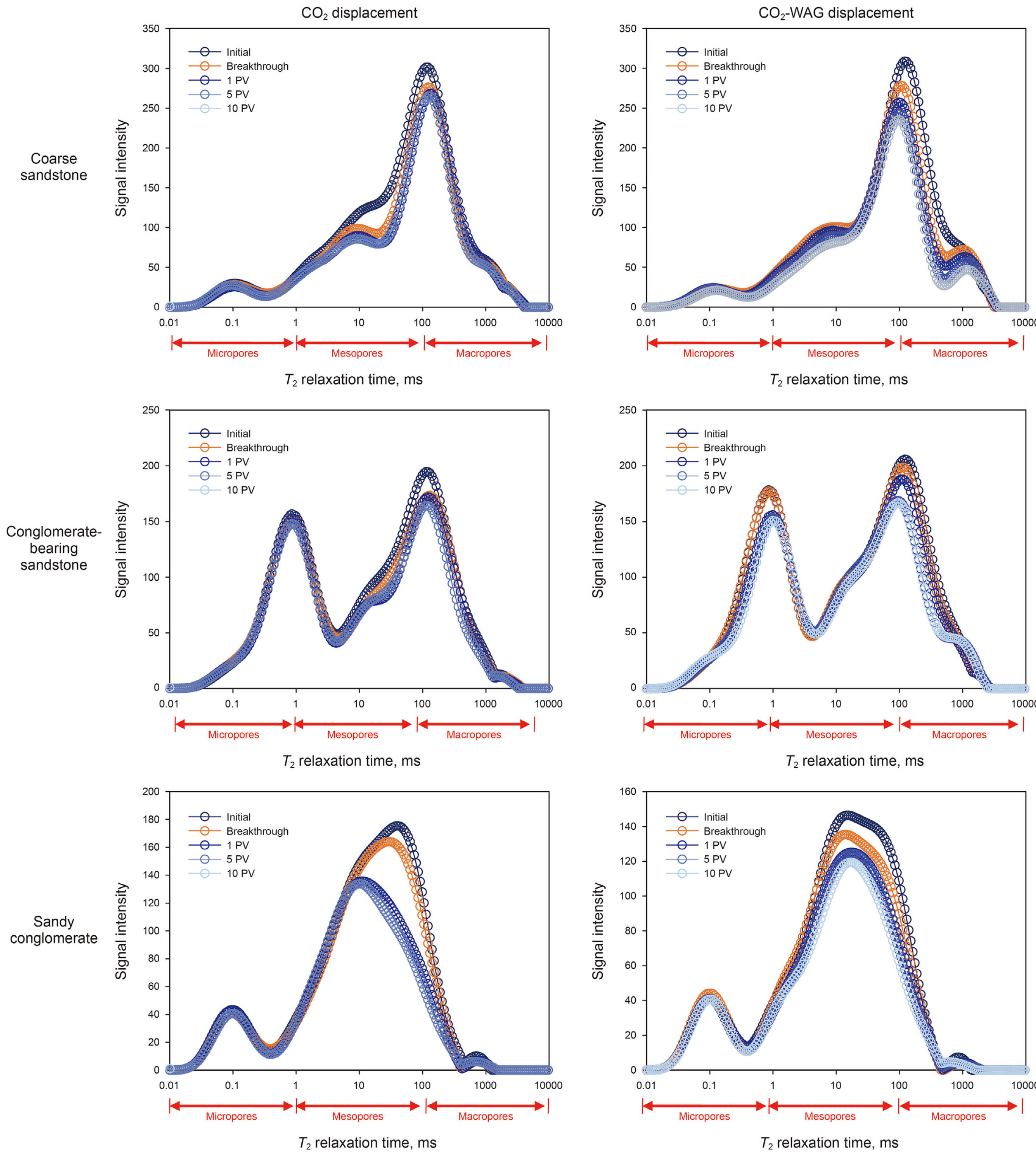

Fig. 6. Dynamic T_2 spectra of three types of cores during CO_2 displacement and CO_2-WAG displacement.

while enhances oil recovery of heterogeneous reservoirs. Notably, the most significant reduction in residual oil saturation was observed in the low-permeability core, which indicates the increased water–gas ratio can improve the utilization efficiency of the low permeability zones.

To further quantify the effect of water–gas ratio on multiscale oil recovery in the CO_2-WAG process, we calculated the oil recovery by integrating T_2 spectral analysis with Eqs. (2) and (4)–(6), as detailed in Figs. 11 and 12. The results illustrate that as the water–gas ratio increases, the total oil recovery rises. The oil

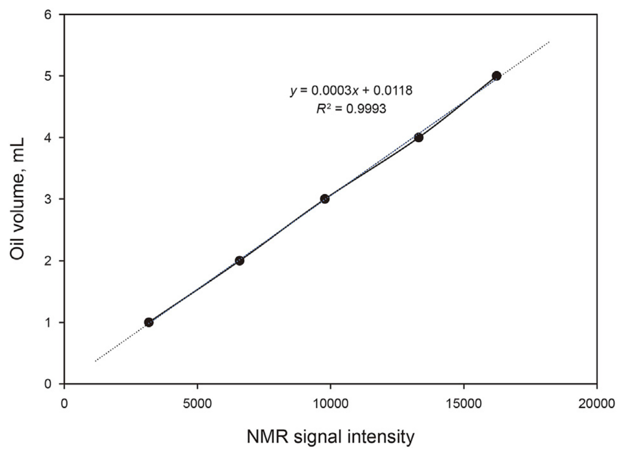

Fig. 7. Relationship between the NMR signal and the oil volume.

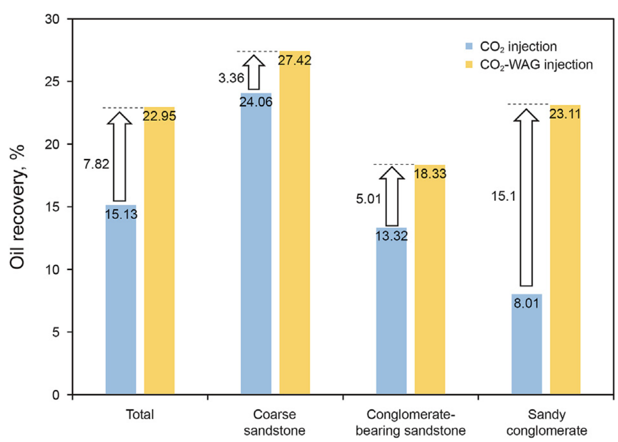

Fig. 8. Total and layer-specific oil recovery after CO_2 and CO_2-WAG (1:1 water–gas ratio) displacement.

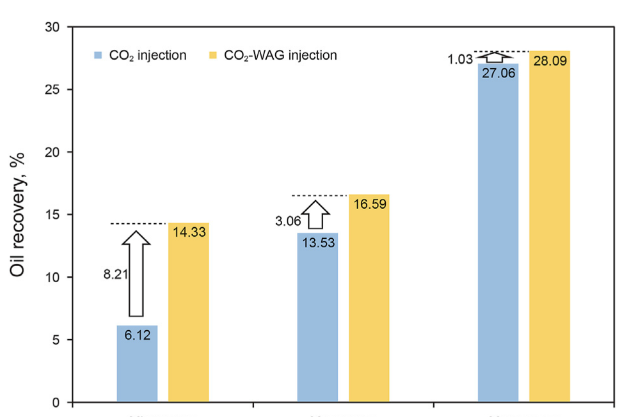

Fig. 9. Oil recovery from three types of pores after CO_2 and CO_2-WAG (1:1 water–gas ratio) displacement.

recovery of heterogeneous reservoirs increases from 23.37% to 25.81%, with an increment up to 2.44%, when the water–gas ratio is increased from 1:2 to 2:1. Especially in the low permeability layer, the oil recovery increased by 5.73% (from 21.96% to 27.69%). By increasing the water–gas ratio, more water can preferentially enter the high permeability layer. Compared with gas, water has higher viscosity and flow resistance, providing a plugging effect in the high-permeability layer, thereby effectively suppressing gas channeling. This encourages gas to divert into the low-permeability layer, resulting in a more uniform fluid distribution and enhanced oil recovery from the low-permeability layer.

On the pore scale analysis, the oil recovery from both macropores and micropores increases as the water–gas ratio rises, with the most significant improvement observed in micropores. This is primarily because higher water–gas ratio increases the overall viscosity of the fluid, resulting in a higher displacement pressure difference. This pressure difference helps to overcome capillary resistance, allowing fluid to enter micropores pores and displace the trapped oil.

While an increase in the water–gas ratio can inhibit gas breakthrough and enhance oil recovery from heterogeneous reservoirs, an excessively high water–gas ratio can reduce injectability. This leads to excessive pressure at the injection end, slow pressure propagation, pressure leakage in the reservoir, and a decrease in oil displacement rate. Therefore, it is crucial to optimize the water–gas ratio by considering multiple factors, including injectability, oil recovery, and production rate. These aspects will be the focus of our follow-up research.

3.1.3. Impact of injection rate on multiscale oil recovery in CO_2-WAG flooding under immiscible condition

To assess the impact of injection rate in CO_2-WAG injection, core displacement experiments were conducted at an injection rate of 0.5, 2, and 5 mL/min. Dynamic NMR images in the process are shown in Fig. 13. As the injection rate increases, gas breakthrough in the high-permeability layer occurs earlier (at 0.39, 0.32, and 0.27 PV, respectively), resulting in higher residual oil saturation, particularly in medium- and low-permeability layers. However, after breakthrough, the higher injection rate is conductive to the enhancement of oil recovery from the medium- and low-permeability layers.

To further quantify this trend, the oil recovery from each layer was calculated using T_2 spectra along with Eqs. (2) and (4)–(6), as illustrated in Fig. 14. The results show that as the injection rate increases, the total oil recovery decreases, while the oil recovery from the low-permeability layer improves. This occurs because a high injection rate causes earlier gas breakthrough in the high-permeability layer, leading to the formation of dominant flow channels, which reduces sweep efficiency and total oil recovery. However, according to Darcy's law, a higher flow velocity generates a larger displacement pressure differential, which helps to overcome the capillary forces in low-permeability layer. This effect becomes especially significant after gas breakthrough.

Moreover, on the pore scale, as shown in Fig. 15, the oil recovery demonstrates that the higher injection rate can significantly improve the oil recovery from micropores, with oil recovery increasing by up to 11.40% (from 2.13% to 13.53%).

Based on the results of this study, the development of heterogeneous reservoirs using CO_2-WAG can be optimized in two stages. Before gas breakthrough, a low injection rate is applied to inhibit gas breakthrough and improve sweep efficiency. After breakthrough, the injection rate should be significantly increased to further reduce the residual oil saturation in medium- and low-permeability layers effectively.

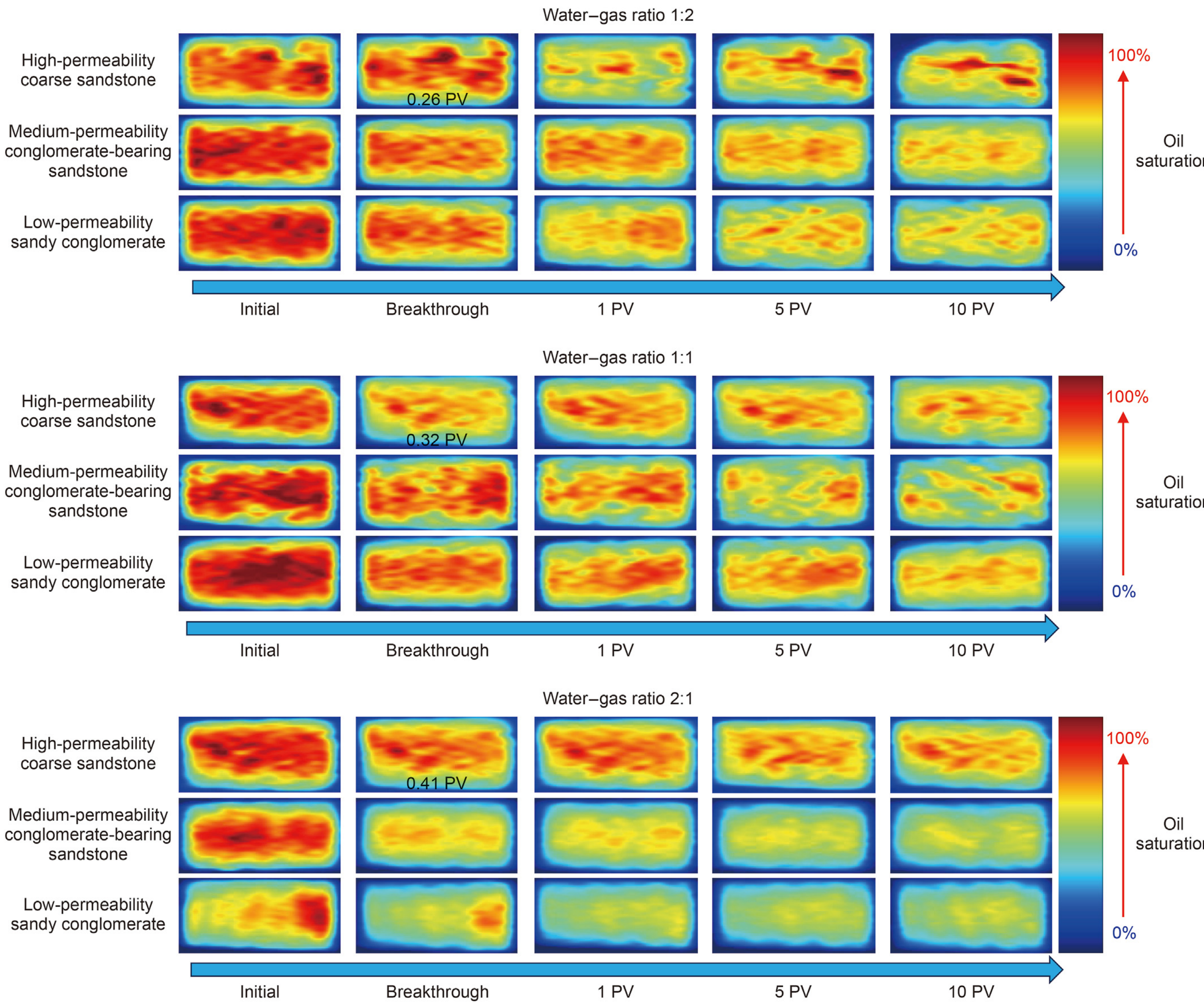

Fig. 10. Dynamic NMR imaging of heterogeneous cores during CO_2-WAG displacement with different water–gas ratios.

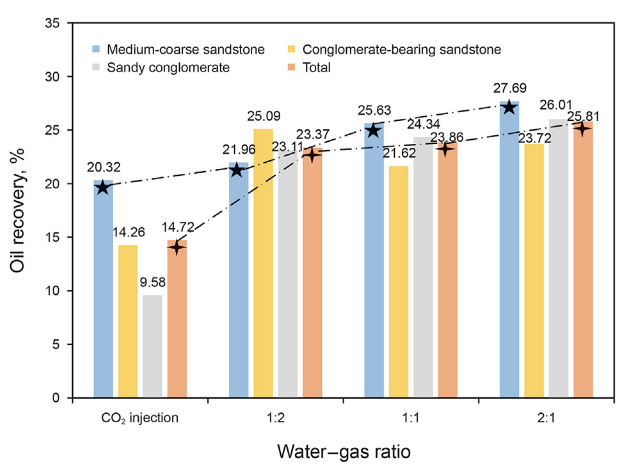

Fig. 11. Total and layer-specific oil recovery after CO_2-WAG displacement with different water–gas ratios.

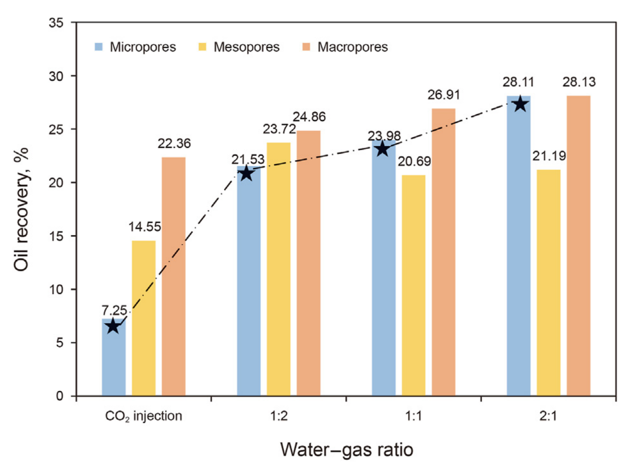

Fig. 12. Oil recovery from three types of pores after CO_2-WAG displacement with different water–gas ratios.

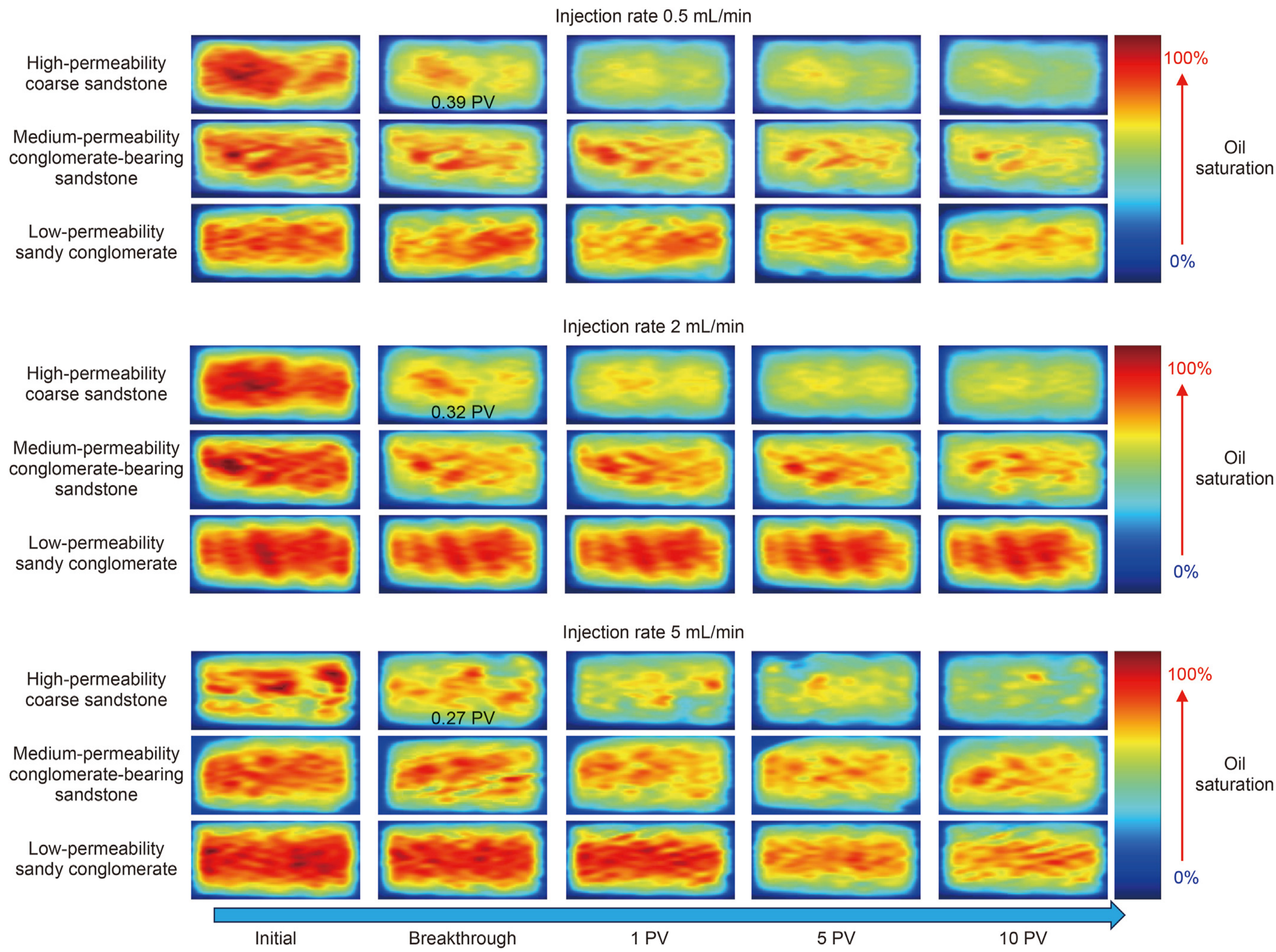

Fig. 13. Dynamic NMR imaging of heterogeneous cores during CO_2-WAG displacement with varying injection rates.

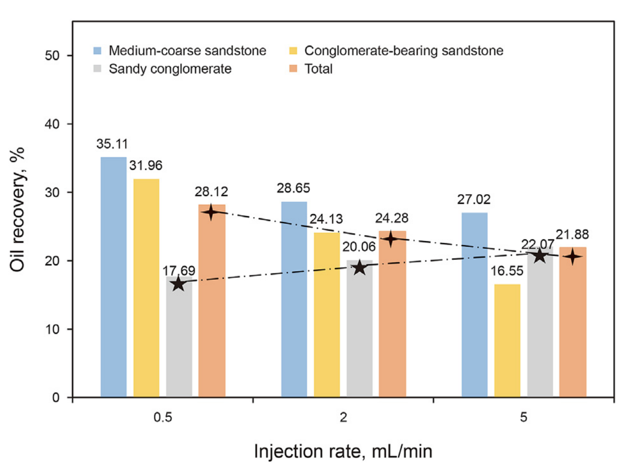

Fig. 14. Total and layer-specific oil recovery after CO_2-WAG displacement with different injection rates.

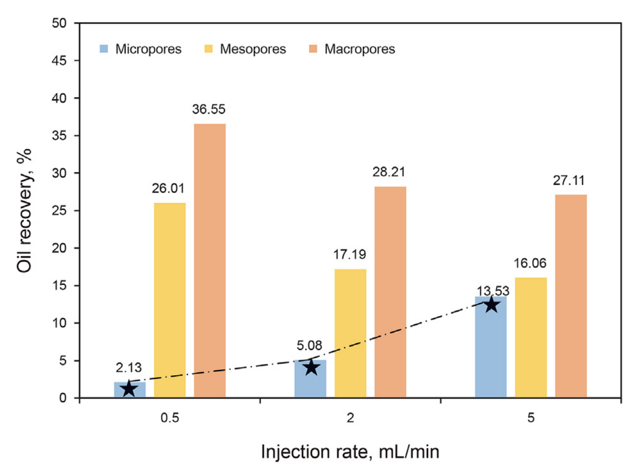

Fig. 15. Oil recovery from three types of pores after CO_2-WAG displacement with different injection rates.

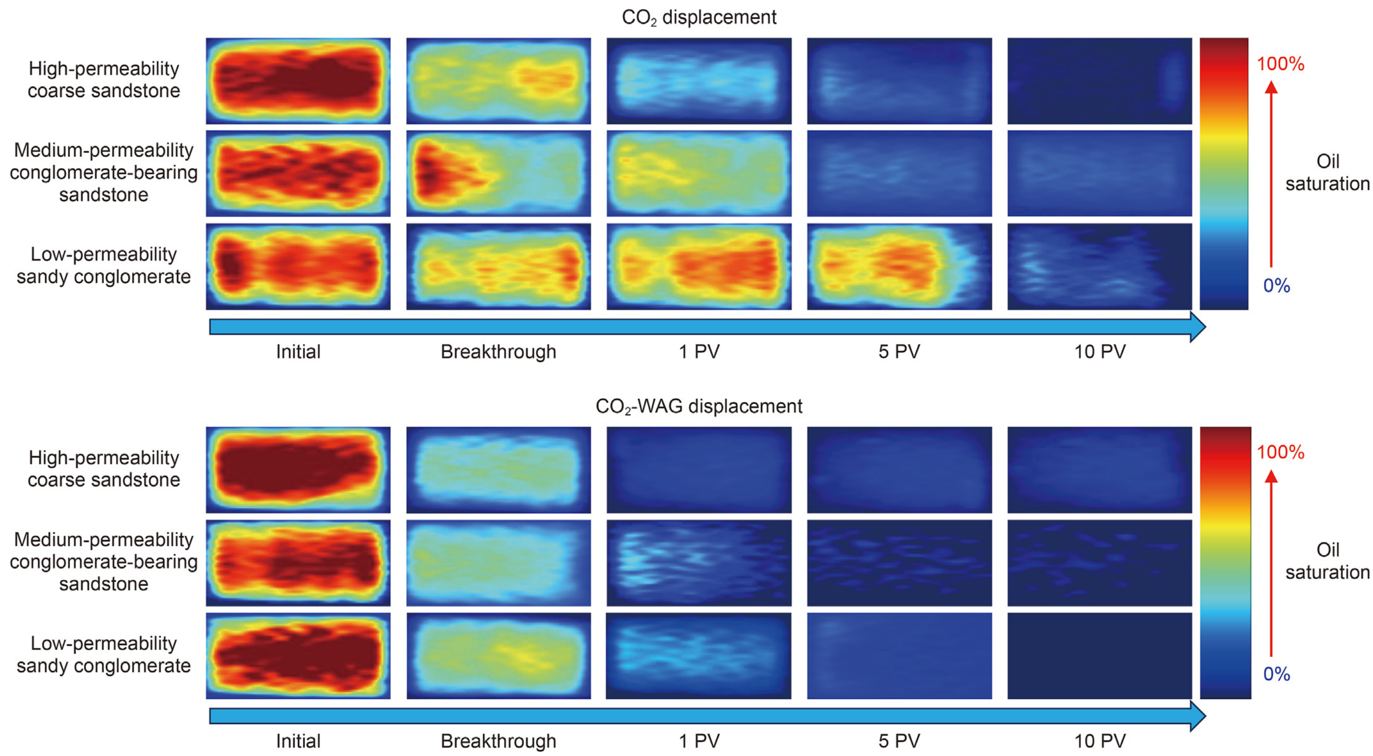

Fig. 16. Dynamic NMR imaging of heterogeneous cores during the CO_2 and CO_2-WAG miscible displacement.

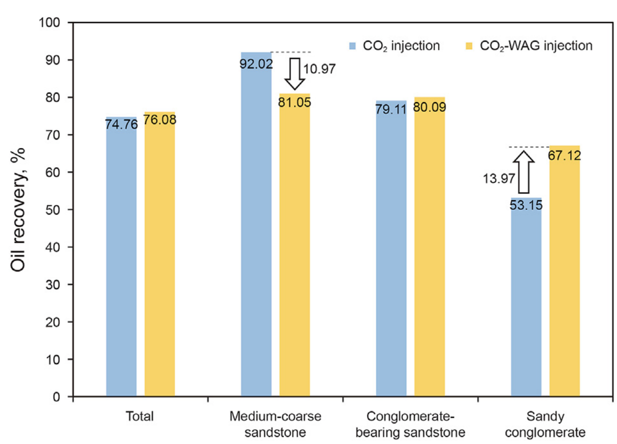

Fig. 17. Total and layer-specific oil recovery after CO_2 displacement and CO_2-WAG (water–gas ratio 1:1) miscible displacement.

3.2. EOR mechanisms and influencing factors for CO_2-WAG flooding under miscible condition

3.2.1. Comparative analysis of recovery performance in CO_2 flooding and CO_2-WAG flooding under miscible condition

In this section, we discuss the effect of CO_2 and CO_2-WAG injection under miscible conditions. Similar to Section 3.1, NMR imaging was used to capture key stages of the displacement process, as shown in Fig. 16. Compared to immiscible displacement (Fig. 5), the residual oil after miscible displacement is significantly reduced at the same injection volume, indicating that miscible displacement can substantially enhance oil recovery. Under miscible conditions, although both displacement methods can ultimately achieve high oil recovery, CO_2-WAG injection yields better results at lower injection volume. However, CO_2 flooding exhibits highly uneven recovery across different layers. In particular, the residual oil in the low-permeability layer is only substantially recovered after 10 PV of CO_2 injection, however, the effect is excellent after 1 PV of CO_2-WAG injection. The results indicate that CO_2-WAG miscible displacement can effectively balance oil recovery across different layers of a heterogeneous reservoir, achieving high oil exchange efficiency. This approach also reduces production time and CO_2 usage.

Similarly, the quantification of oil recovery for different displacement modes was conducted as described in Section 3.1, with the results presented in Fig. 17. In the miscible state, the total oil recovery of the heterogeneous cores is approximately 75%, which is 3–9 times higher than that of immiscible flooding. In terms of total oil recovery, there is minimal difference between CO_2 injection and CO_2-WAG injection. However, CO_2-WAG injection can enhance the oil recovery from the low-permeability sandy conglomerate layer to some extent and help balance the recovery across different layers.

In addition, oil recovery on the pore scale is illustrated in Fig. 18. Under miscible conditions, the oil recovery from three types of pore still decreases as follows: macropores, mesopores, micropores. This reduction is due to the pronounced wall effect and increased flow resistance in micropores. Additionally, the confinement effect in micro- and nanoscale pores results in high miscible pressure, causing CO_2 and crude oil to remain in an immiscible state within micropores (Sun et al., 2024). This leads to increased interfacial tension between CO_2 and crude oil, resulting in significant oil entrapment due to capillary resistance. Compared with the CO_2 displacement, the CO_2-WAG displacement can enhance the oil recovery from micropores and mesopores by up to 10.33% and 14.29%,

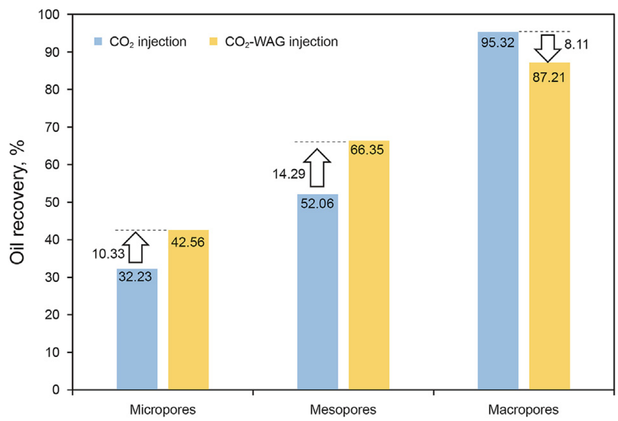

Fig. 18. Oil recovery from three types of pores after CO_2 displacement and CO_2-WAG displacement (water–gas ratio 1:1).

respectively. CO_2-WAG also helps to balance oil recovery on the pore scale. However, compared to macropores the recovery rate in micropores and mesopores remains significantly lower. Therefore, effectively enhancing oil recovery from micropores remains a key challenge in the development of heterogeneous sandy conglomerate reservoirs using CO_2 injection.

3.2.2. *Impact of water–gas ratio on multiscale oil recovery in CO_2-WAG flooding under miscible condition*

To investigate the impact of water–gas ratios on oil recovery during the CO_2-WAG process under miscible conditions, NMR imaging was conducted at the same key stages of the process (as described in Section 3.1). The results are presented in Fig. 19. Experimental results indicate that an increase in water–gas ratio can enhance oil recovery from low-permeability layers, particularly at low injection volume. At the high injection volume, most of the residual oil has already been displaced. The calculated oil recovery results are shown in Fig. 20, indicating that the final oil recovery is

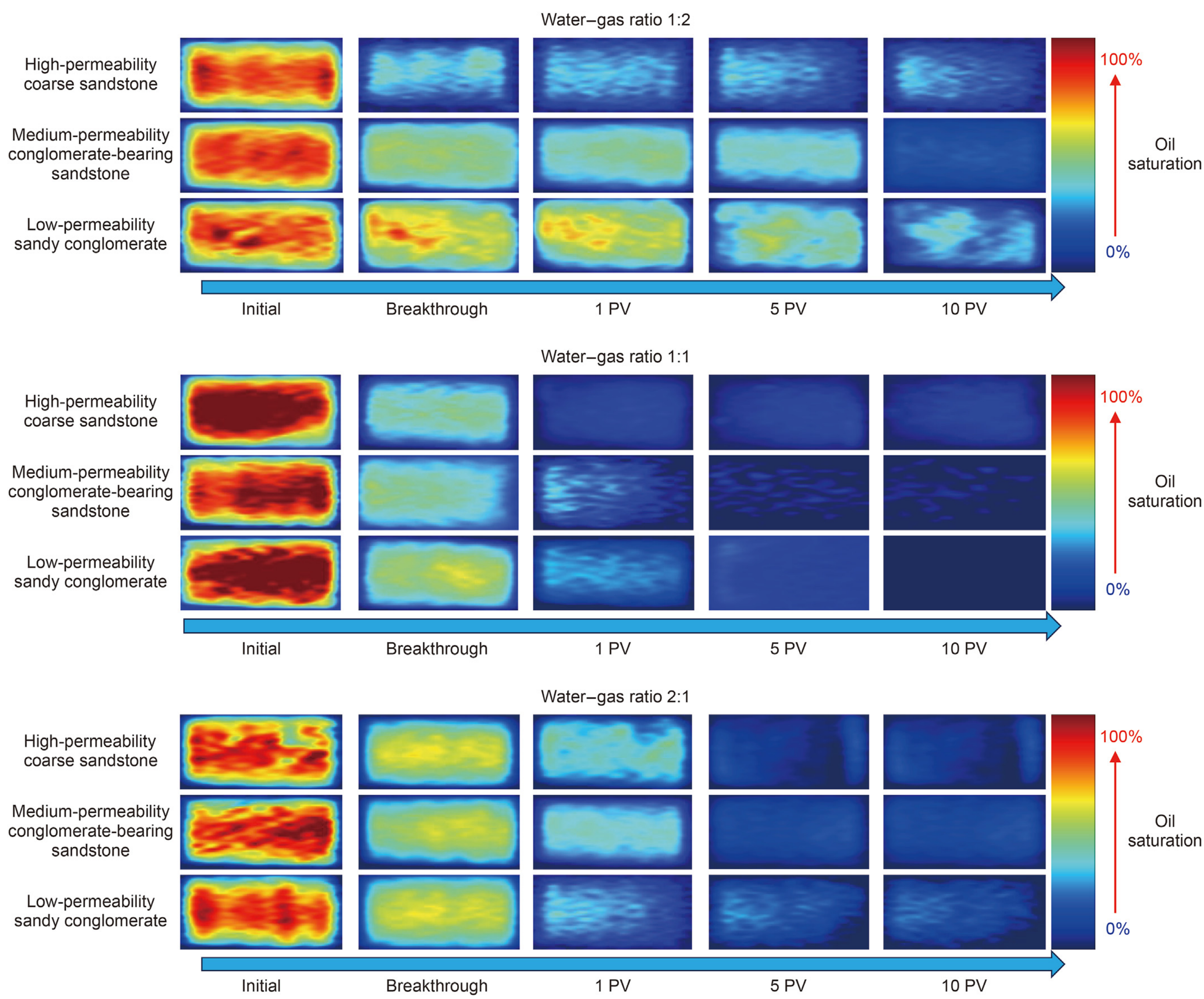

Fig. 19. Dynamic NMR imaging of heterogeneous cores during CO_2-WAG miscible displacement with different water–gas ratios.

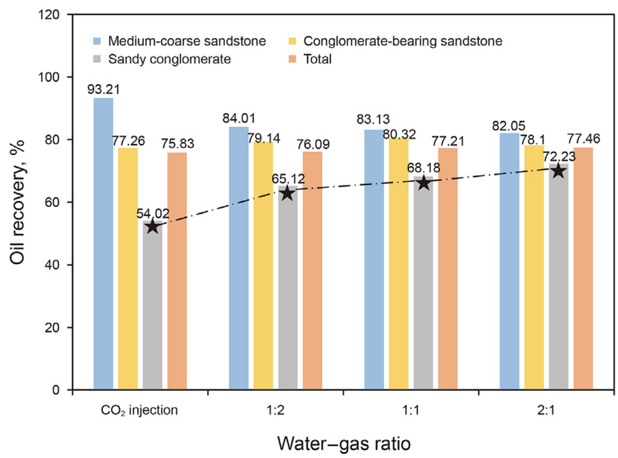

Fig. 20. Total and layer-specific oil recovery after CO_2-WAG miscible displacement with different water–gas ratios.

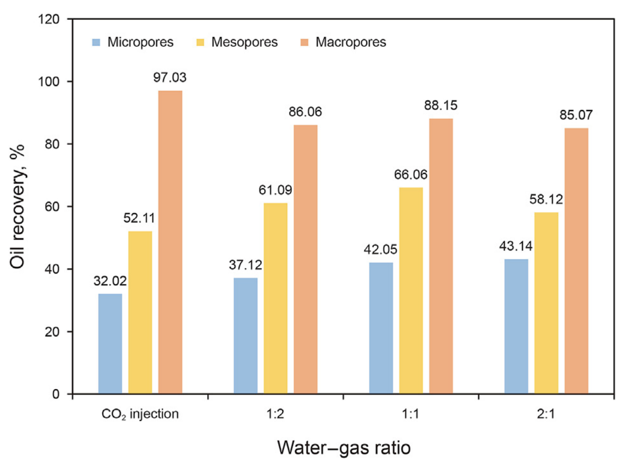

Fig. 21. Oil recovery from three types of pores after CO_2-WAG miscible displacement with different water–gas ratios.

around 80% across different water–gas ratios. Furthermore, the oil recovery from each layer was also found to be relatively insensitive to changes in the water–gas ratio. On the pore scale, as shown in Fig. 21, the oil recovery in the miscible state improves significantly. However, adjusting the water–gas ratio had no notable effect on the oil recovery in this state.

In general, under miscible conditions, the water–gas ratio has minimal impact on the oil production of heterogeneous sandy conglomerate reservoirs at high injection volume. However, on a reservoir scale, injecting multiple volume of displacing fluid consumes a significant amount of CO_2 and water. Therefore, moderately increasing the water–gas ratio can achieve a higher swept area and improved displacement efficiency with a smaller injection volume. Conversely, excessively increasing the water–gas ratio can reduce injectability and hinder the miscibility of CO_2 and crude oil, ultimately compromising enhanced oil recovery in the reservoir.

3.2.3. Impact of injection rates on multiscale oil recovery in CO_2-WAG flooding under immiscible condition

The impact of injection rate on oil recovery during the CO_2-WAG process under miscible conditions was also investigated by the above-mentioned methods. The results, with injection rates ranging from 0.5 to 5 mL/min, recorded by the NMR imaging are shown in Fig. 22. It was observed that during the early stages of CO_2-WAG injection, the oil recovery from low-permeability layers could be enhanced. After the high injection volume, most of the residual oil was recovered, leaving only a small amount of oil trapped in the core. Similar to the previous analysis, the total and layer-specific oil recovery after CO_2-WAG were quantified, as shown in Fig. 23. The total oil recovery remained around 77% at different injection rates, and the change of injection rate has little effect on the recovery rate of each layer. In addition, on the pore scale, as shown in Fig. 24, under miscible conditions the injection rate has little effect on the oil recovery from three types of pores.

In summary, under miscible conditions, altering the injection rate during high injection volume has minimal impact on the oil recovery from heterogeneous sandy conglomerate reservoirs. However, in practical reservoir applications, increasing the injection rate appropriately in the early stage of injection can enhance oil recovery from low-permeability layers and improve overall sweep efficiency. Initially, a higher injection rate can quickly establish a higher reservoir pressure, facilitating deeper penetration of CO_2 and water into low-permeability zones. This rapid pressure buildup allows for a more uniform distribution of CO_2 and water across the reservoir, particularly impacting the lower permeability layers in the early stages. As the displacement process progresses, the fluid distribution and pressure field within the reservoir gradually reach a new equilibrium, resulting in similar ultimate oil recovery at different injection rates. However, excessively increasing the injection rate might lead to rapid local pressure buildups, increasing the risk of reservoir fracturing, and could also cause water coning or gas breakthrough. Excessive injection of CO_2 and water also escalates costs.

Therefore, it is crucial in practical operations to find a balanced displacement strategy to achieve optimal hydrocarbon recovery efficiency and economic benefits.

4. Conclusions

In this study, a high-temperature and high-pressure online NMR experimental system was established. A multiscale (reservoir-layer-pore) approach was developed to investigate the EOR mechanisms of CO_2 flooding/CO_2-WAG flooding in heterogeneous sandy conglomerate reservoirs. The mechanisms for enhanced oil recovery under both miscible and immiscible conditions were revealed, and the effects of factors such as injection rate and water–gas ratio on oil recovery were clarified. The findings provide recommendations for the sustained and efficient development of heterogeneous sandy conglomerate reservoirs. The main conclusions are as follows:

(1) In the immiscible state, CO_2-WAG enhances oil recovery compared to gas flooding primarily by delaying CO_2 breakthrough in high-permeability layers and improving oil recovery in medium- and low-permeability layers. Additionally, this method boosts oil displacement efficiency in mesopores and micropores, which provides a new perspective for understanding the micro-mechanisms of CO_2-WAG flooding.
(2) In the immiscible CO_2-WAG flooding state, the appropriate increases in water–gas ratio and injection rate are conducive to oil recovery in low–permeability layers and micropores.

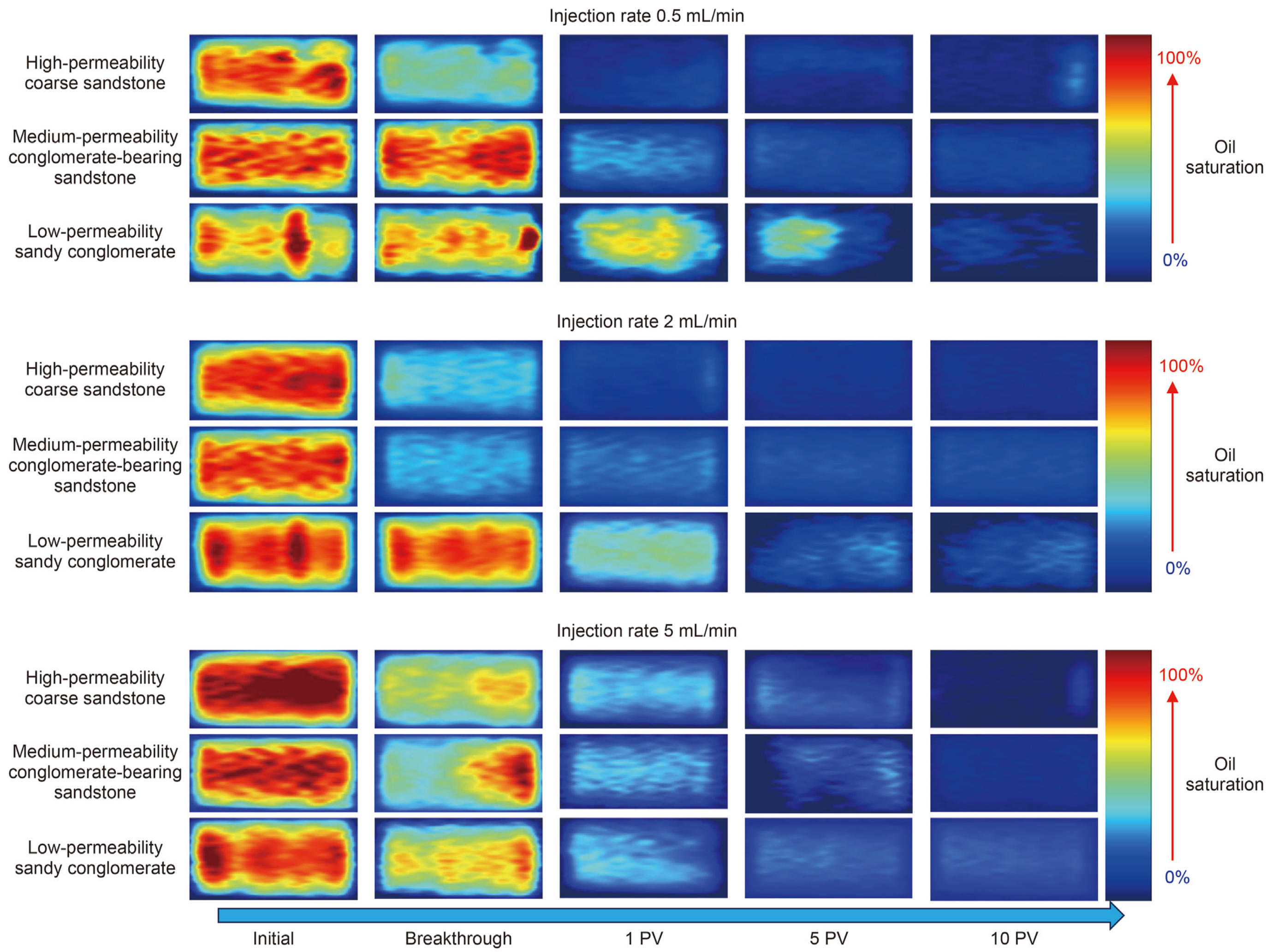

Fig. 22. Dynamic NMR imaging of heterogeneous cores during CO_2-WAG miscible displacement with varying injection rates.

However, how to optimize the water–gas ratio and injection rate needs to be further simulated on the reservoir scale.

(3) In the miscible state, CO_2-WAG flooding can significantly enhance oil recovery and contribute to balancing the oil recovery efficiency from different types of pores. Then, maintaining high formation pressure can enhance the oil recovery from heterogenous reservoirs, but it can reduce the

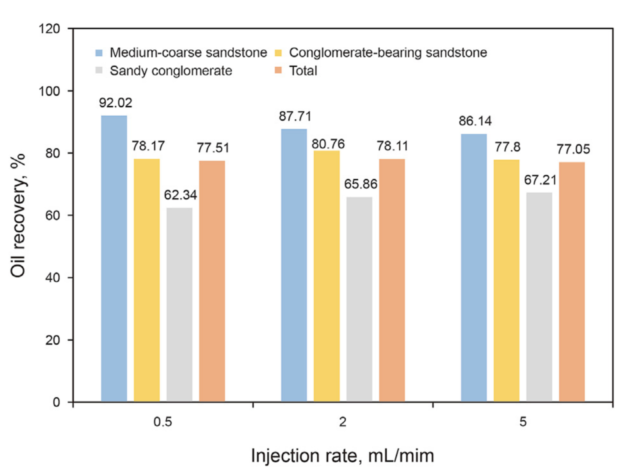

Fig. 23. Total and layer-specific oil recovery after CO_2-WAG miscible displacement with different injection rates.

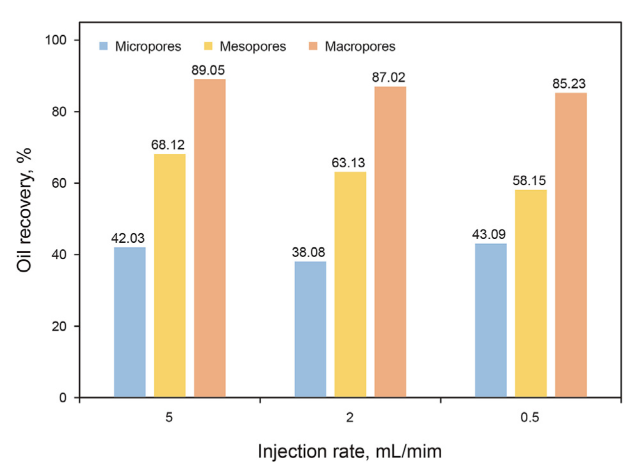

Fig. 24. Oil recovery from three types of pores after CO_2-WAG miscible displacement with different injection rates.

oil production rate. Therefore, development strategies should be adjusted based on site requirements.

(4) In the miscible state, the water–gas ratio and injection rate have minimal impact on the oil recovery on the core scale. However, on the reservoir scale, the effects of these parameters on oil recovery require further investigation.

CRediT authorship contribution statement

Jun-Rong Liu: Writing – review & editing, Writing – original draft, Methodology, Formal analysis, Conceptualization. **Deng-Feng Zhang:** Writing – review & editing, Writing – original draft, Visualization, Formal analysis, Data curation. **Shu-Yang Liu:** Writing – review & editing, Supervision, Project administration, Methodology, Funding acquisition. **Run-Dong Gong:** Visualization, Methodology, Investigation. **Li Wang:** Writing – review & editing.

Declaration of competing interest

The authors declare that they have no known competing financial interests or personal relationships that could have appeared to influence the work reported in this paper.

Acknowledgments

This paper was financially supported by the National Natural Science Foundation of China (No. 52204065, No. 52374063), the Independent Innovation Research Project of China University of Petroleum (No. 24CX06017A), and Shandong Provincial Natural Science Foundation, China (No. ZR2024QE075, No. ZR2023ME049).

References

Afzali, S., Rezaei, N., Zendehboudi, S., 2018. A comprehensive review on enhanced oil recovery by water alternating gas (WAG) injection. Fuel 227, 218–246. https://doi.org/10.1016/j.fuel.2018.04.015.

Al-Saedi, H.N., Long, Y., Flori, R.E., et al., 2019. Coupling smart seawater flooding and CO_2 flooding for sandstone reservoirs: smart seawater alternating CO_2 flooding (SMSW-AGF). Energy Fuel. 33 (10), 9644–9653. https://doi.org/10.1021/acs.energyfuels.9b02289.

Cai, M., Su, Y., Hao, Y., et al., 2021. Monitoring oil displacement and CO_2 trapping in low-permeability media using NMR: a comparison of miscible and immiscible flooding. Fuel 305, 121606. https://doi.org/10.1016/j.fuel.2021.121606.

Chen, H., Yang, S., Liu, J., et al., 2016. Experimental study on injection strategy of CO_2 near-miscible flooding in low permeability reservoirs with high water cut. In: International Petroleum Technology Conference. https://doi.org/10.2523/IPTC-18770-MS.

Chen, S., Li, H., Yang, D., et al., 2010. Optimal parametric design for water-alternating-gas (WAG) process in a CO_2-miscible flooding reservoir. J. Can. Petrol. Technol. 49 (10), 75–82. https://doi.org/10.2118/141650-PA.

Cui, M., Wang, R., Lun, Z., et al., 2022. Characteristics of water alternating CO_2 injection in low-permeability beach-bar sand reservoirs. Energy Geosci. 2022, 100119. https://doi.org/10.1016/j.engeos.2022.06.007.

Du, D., Pu, W., Jin, F., et al., 2020. Experimental study on EOR by CO_2 huff-n-puff and CO_2 flooding in tight conglomerate reservoirs with pore scale. Chem. Eng. Res. Des. 156, 425–432. https://doi.org/10.1016/j.cherd.2020.02.018.

Guo, D.B., Xu, H.M., 2014. Laboratory experiments of CO_2 flooding in deep-buried high-pressure low-permeability reservoirs: a case study of block Hu96 in Zhongyuan Oilfield. Exp. Pet. Geol. 36 (1), 102–105. https://doi.org/10.11781/sysydz201401102 (in Chinese).

Henni, A., 2014. Technology could cut CO_2 cost sharply for enhanced oil recovery. J. Petrol. Technol. 66 (6), 30–32. https://doi.org/10.2118/0614-0030-JPT.

Hu, Y.L., Hao, M.Q., Chen, G.L., 2019. Technology and practice of CO_2 flooding and storage in China. Petrol. Explor. Dev. 46 (4), 716–727 (in Chinese).

Jiang, Z., Tang, H., Wang, J., et al., 2023. Characterization of extra low-permeability conglomerate reservoir and analysis of three-phase seepage law. Processes 11 (7), 2054. https://doi.org/10.3390/pr11072054.

Kulkarni, M.M., Rao, D.N., 2005. Experimental investigation of miscible and immiscible Water-Alternating-Gas (WAG) process performance. J. Petrol. Sci. Eng. 48 (1–2), 1–20. https://doi.org/10.1016/j.petrol.2005.05.001.

Lan, Y., Yang, Z., Wang, P., et al., 2019. A review of microscopic seepage mechanism for shale gas extracted by supercritical CO_2 flooding. Fuel 238, 412–424. https://doi.org/10.1016/j.fuel.2018.10.130.

Liu, J., Li, H., Liu, S., et al., 2023. Investigating the impact of aqueous phase on CO_2 Huff 'n'Puff in tight oil reservoirs using nuclear magnetic resonance technology: stimulation measures and mechanisms. SPE J. 28 (6), 3324–3340. https://doi.org/10.2118/217978-PA.

Liu, S., Li, H., Zhang, K., et al., 2022a. Techno-economic analysis of using carbon capture and storage (CCS) in decarbonizing China's coal-fired power plants. J. Clean. Prod. 351, 131384. https://doi.org/10.1016/j.jclepro.2022.131384.

Liu, S.Y., Ren, B., Li, H.Y., et al., 2022b. CO_2 storage with enhanced gas recovery (CSEGR): a review of experimental and numerical studies. Pet. Sci. 19 (2), 594–607. https://doi.org/10.1016/j.petsci.2021.12.009.

Liu, X., Ma, L., Tan, J., et al., 2017. CO_2-EOR in fractured ultra-low permeability reservoirs: problems and remedial measures. In: Carbon Management Technology Conference. https://doi.org/10.7122/486671-MS.

Masalmeh, S., Farzaneh, S.A., Sohrabi, M., et al., 2022. A systematic experimental study to understand the performance and efficiency of gas injection in carbonate reservoirs. SPE Reservoir Eval. Eng. 26 (4), 1159–1174. https://doi.org/10.2118/200057-PA.

Nezhad, S.A.T., Mojarad, M.R.R., Paitakhti, S.J., et al., 2006. Experimental study on applicability of water-alternating-CO_2 injection in the secondary and tertiary recovery. In: SPE International Oil Conference and Exhibition in Mexico. https://doi.org/10.2118/103988-MS.

Odesa, D., 2018. The challenges and lessons of enhanced oil recovery using sequestrated CO_2. In: SPE Nigeria Annual International Conference and Exhibition. https://doi.org/10.2118/193379-MS.

Qian, K., Yang, S.L., Dou, H.E., 2019. Experimental study on fluid property change and oil displacement mechanism during CO_2 injection. Bulletin Petrol. Sci. 4 (1), 69 (in Chinese).

Ramachandran, K.P., Gyani, O.N., Sur, S., 2010. Immiscible hydrocarbon WAG: laboratory to field. In: SPE Oil and Gas India Conference and Exhibition. https://doi.org/10.2118/128848-MS.

Singh, H., 2018. Impact of four different CO_2 injection schemes on extent of reservoir pressure and saturation. Adv. Geo-Energy Res. 2 (3). https://doi.org/10.26804/ager.2018.03.08.

Sun, Q., Zhang, N., Zhu, P., et al., 2024. Confined fluid interfacial tension and minimum miscibility pressure prediction in shale nanopores. Fuel 364, 130949. https://doi.org/10.1016/j.fuel.2024.130949.

Tian, W., Lu, S., Zhang, J., et al., 2022. NMR characterization of fluid mobility in low-permeability conglomerates: an experimental investigation of spontaneous imbibition and flooding. J. Petrol. Sci. Eng. 214, 110483. https://doi.org/10.1016/j.petrol.2022.110483.

Toumelin, E., Torres-Verdín, C., Sun, B., et al., 2007. Random-walk technique for simulating NMR measurements and 2D NMR maps of porous media with relaxing and permeable boundaries. J. Magn. Reson. 188 (1), 83–96. https://doi.org/10.1016/j.jmr.2007.05.024.

Wang, Y.F., Li, Z.Y., Zhang, S.M., 2021. Residual oil distribution after CO_2/water/gas injection in different heterogeneous models: a visualization study by NMR. J. Cent. S. Univ. 28 (5), 1412–1421 (in Chinese).

Wang, Y.N., Wu, X.D., Zhan, Z.Y., 2013. Experiment of alternating water and gas flooding in low permeability and high water cut reservoir. Gasf. Surf. Eng. 32 (11), 43–44 (in Chinese).

Wang, Z., Lin, B., Chen, G., et al., 2023. Experimental study on evaluation of conglomerate reservoir support-type fracture conductivity in Xinjiang oilfield. Energy 278, 127877. https://doi.org/10.1016/j.energy.2023.127877.

Xu, T., Tian, H., Zhu, H., et al., 2022. China actively promotes CO_2 capture, utilization and storage research to achieve carbon peak and carbon neutrality. Adv. Geo-Energy Res. 6 (1), 1–3. https://doi.org/10.46690/ager.2022.01.01.

Yu, Z., Wang, Z., Jiang, Q., et al., 2022. Evaluation of low permeability conglomerate reservoirs based on petrophysical facies: a case study from the Triassic Baikouquan Formation, northern Mahu Sag, Junggar Basin, China. J. Petrol. Sci. Eng. 219, 111082. https://doi.org/10.1016/j.petrol.2022.111082.

Zhang, L., Nowak, W., Oladyshkin, S., et al., 2023. Opportunities and challenges in CO_2 geologic utilization and storage. Adv. Geo-Energy Res. 8 (3). https://doi.org/10.46690/ager.2023.06.01.

Zhao, C., Song, Z., Yao, Y., et al., 2019. Effect of water-alternating-gas injection on gas and water production control in carbonate reservoirs. In: Carbon Management Technology Conference. https://doi.org/10.7122/CMTC-558862-MS.